Two-Dimensional [TIn_2] Polyanions in $BaTIn_2$ (T = Rh, Pd, Ir, Pt)—The Collapse of the Three-Dimensional Indium Polyanion of $BaIn_2$

Rolf-Dieter Hoffmann and Rainer Pöttgen*[a]

Abstract: The title compounds were prepared from the elements by reactions in sealed tantalum tubes in a high-frequency furnace. The four compounds were investigated by X-ray diffraction both on powders and single crystals, and the structures of the rhodium and platinum compounds were refined from single-crystal data: *Cmcm*, $a = 447.68(8)$, $b = 1131.1(2)$, $c = 805.6(2)$ pm, $wR2 = 0.0561$, 354 F^2 values for $BaRhIn_2$; $a = 452.06(8)$, $b = 1162.4(2)$, $c = 801.5(1)$ pm, $wR2 = 0.1427$, 362 F^2 values, for $BaPtIn_2$: with 16 variables for each refinement. The structures are isopointal to $MgCuAl_2$ and can be considered to be a transition metal (T) filled $CaIn_2$ type, in which the indium atoms form a distorted network like hexagonal diamond (lonsdaleite). The indium substructure is cut apart in $BaTIn_2$ and resembles together with the transition metal atoms a two-dimensional polyanion rather than a three-dimensional polyanion as found in the compounds $CaTIn_2$, $CaTSn_2$, and $SrTIn_2$. Semiempirical band structure calculations support the assumption of a two-dimensional polyanion in which the strongest interactions are found for the T–In contacts.

Keywords: barium · chemical bonding · indium · polyanions · structure elucidation

Introduction

The crystal structure and chemical bonding of the alkaline earth indides and stannides $CaTIn_2$ (T = Ni, Cu, Rh, Pd, Ir, Pt, Au),[1–4] $CaTSn_2$ (T = Rh, Pd, Ir),[5] and $SrTIn_2$ (T = Rh, Pd, Ir, Pt)[6] have been investigated intensively in recent years. From a purely geometrical point of view, these structures may be derived from the Re_3B type[7] by an ordered arrangement of the alkaline earth and indium atoms on the rhenium site, while the transition metal atoms take the boron position. This is actually the $MgCuAl_2$ type.[8]

As emphasized previously,[4–6] the crystal-chemical description of the $CaTIn_2$ and $SrTIn_2$ compounds as transition metal filled variants of the Zintl phases $CaIn_2$[9] and $SrIn_2$[9] is more appropriate. The transition metal atoms tend to fill their *d* bands and hence they partially oxidize the indium networks to meet their electronic requirements. This is especially true for the isotypic stannides $CaTSn_2$.[5] This oxidation results in a modulation of the In–In distances within the indium network depending on the electron count of the transition metal.[4–6] The indium atoms and the transition metal atoms build three-dimensional [TIn_2] polyanions, and the resulting distorted pentagonal channels in these networks are filled by calcium or strontium atoms.

Within the series of the binary indides a structural switch occurs in going from $SrIn_2$[9] to $BaIn_2$.[10, 11] While $SrIn_2$ still crystallizes with the hexagonal $CaIn_2$-type structure, $BaIn_2$ adopts the orthorhombic KHg_2[12] ($CeCu_2$[13]) type with larger cavities for the barium cations. Nevertheless, the new compounds $BaTIn_2$ (T = Rh, Pd, Ir, Pt) reported here are transition metal filled versions of a $CaIn_2$-type $BaIn_2$ substructure. The size requirements are solved in a way that the large barium atoms cut the three-dimensional indium network of $BaIn_2$ and we observe now two-dimensional [TIn_2] polyanions which are separated by barium cations.

[a] Prof. Dr. R. Pöttgen, Dr. R.-D. Hoffmann
Department Chemie
Ludwig-Maximilians-Universität München
Butenandtstrasse 5-13 (Haus D)
81377 München (Germany)
Fax: (+49) 89 2180-7431
E-mail: rapch@cup.uni-muenchen.de

Experimental Section

Synthesis: Starting materials for the preparation of $BaTIn_2$ (T = Rh, Pd, Ir, Pt) were barium rods (Johnson Matthey, >99.9%), rhodium, palladium, iridium, platinum powder (Degussa, 200 mesh, >99.9%), and indium tear drops (Johnson Matthey, >99.9%). The large barium rods were cut into small pieces under paraffin oil and subsequently washed with *n*-hexane. The paraffin oil and *n*-hexane were dried over sodium wire. The compact barium pieces were stored in Schlenk tubes under argon prior to the reactions. The argon was purified over titanium sponge (900 K), silica gel, and molecular sieves.

The barium pieces (about 500 mg) were subsequently mixed with the noble metal and indium pieces in the ideal 1:1:2 atomic ratio and sealed in tantalum tubes (about 1 cm^3) under an argon pressure of about 800 mbar.[14] The tantalum tubes were put in a water-cooled quartz glass sample

0947-6539/01/0702-0382 $ 17.50+.50/0 *Chem. Eur. J.* **2001**, *7*, No. 2

chamber of a high-frequency furnace (Kontron Roto-Melt, 1.2 kW) under flowing argon.[15] They were first heated for two minutes with the maximum power output (about 1500 K) and subsequently annealed at about 900 K for another four hours. The tubes were finally quenched by radiative heat loss within the water-cooled sample chamber. The reaction between the three elements was visible by a short glowing of the tubes. After the annealing procedures the light-gray samples could readily be separated from the tantalum tubes. No reactions of the samples with the tubes could be detected. The samples are slightly moisture sensitive as compact buttons and highly moisture sensitive as fine-grained powders. Single crystals exhibit metallic luster.

The hydrolysis behavior can be attributed to the presence of a two-dimensional polyanion in $BaTIn_2$ in contrast to the three-dimensional polyanion in $CaTIn_2$,[1–4] $CaTSn_2$,[5] and $SrTIn_2$.[6] The latter compounds are all stable in moist air. One can assume that water attacks the barium layers more easily, because of the two-dimensional character of the polyanion. A similar hydrolysis behavior has been found for $Sr_2Rh_2In_3$ which also has a pronounced two-dimensional polyanion.[16] The shape of the $BaTIn_2$ crystals mirrors the two-dimensional character of the polyanion, too. The calcium and strontium compounds have a more globular shape, but crystals of $BaTIn_2$ grow in the form of very thin platelets which can be cleaved easily. This is consistent with the many crystals found of extremely poor quality and extensive diffuse streaks in the reciprocal lattice especially for $BaPdIn_2$ and $BaIrIn_2$. The isotypic stannide $BaRhSn_2$ displays even poorer crystallinity.[17]

Energy-dispersive analyses revealed in all cases the ideal composition of 1:1:2. No impurity elements heavier than sodium could be detected.

X-ray investigations: Guinier powder patterns of the samples were recorded with $Cu_{K\alpha 1}$ radiation using α-quartz ($a = 491.30$, $c = 540.46$ pm) as an internal standard. The orthorhombic lattice constants (see Table 1) were obtained from least-squares fits of the Guinier data. To ensure correct indexing the observed patterns were compared with calculated ones[18] taking the atomic positions from the structure refinements. To calculate the powder pattern correctly for $BaIrIn_2$ and $BaPdIn_2$, the atomic positions of $BaRhIn_2$ and $BaPtIn_2$ were used, respectively. In all cases the lattice constants determined from the powders and the single crystals agreed well. Single crystal intensity data were collected at room temperature by use of a four-circle diffractometer (CAD4) with graphite-monochromated $Mo_{K\alpha}$ radiation ($\lambda = 0.71073$ pm) and a scintillation counter with pulse height discrimination. The scans were performed in the $\omega/2\theta$ mode. Empirical absorption corrections were applied on the basis of psi-scan data.

Table 1. Lattice parameters of orthorhombic barium compounds $BaTIn_2$ (T = Rh, Pd, Ir, Pt).

Compound	a (pm)	b (pm)	c (pm)	V (nm^3)
$BaRhIn_2$	447.68(8)	1131.1(2)	805.6(2)	0.4079
$BaPdIn_2$	457.39(8)	1153.4(4)	803.4(1)	0.4238
$BaIrIn_2$	443.41(8)	1150.7(2)	806.4(1)	0.4115
$BaPtIn_2$	452.06(8)	1162.4(2)	801.5(1)	0.4212

Abstract in German: *Die Titelverbindungen wurden durch Reaktion der Elemente in geschlossenen Tantalampullen in einem Hochfrequenzofen hergestellt und röntgenographisch an Pulvern und Einkristallen charakterisiert. Die Strukturen der Rhodium- und Platinverbindung wurden verfeinert: Cmcm, $a = 447.68(8)$, $b = 1131.1(2)$, $c = 805.6(2)$ pm, $wR2 = 0.0561$, 354 F^2 Werte für $BaRhIn_2$ und $a = 452.06(8)$, $b = 1162.4(2)$, $c = 801,5(1)$ pm, $wR2 = 0.1427$, 362 F^2 Werte für $BaPtIn_2$ mit jeweils 16 Variablen. Die Strukturen sind punktlagengleich zu $MgCuAl_2$ und können als ein mit Übergangsmetall gefülltes $CaIn_2$ aufgefasst werden, in dem die Indium Atome ein verzerrtes Netzwerk bilden wie in hexagonalem Diamant (Lonsdaleit). Die Indium Substruktur ist aufgebrochen und bildet zusammen mit den Übergangsmetall Atomen ein zweidimensional unendliches Polyanion im Gegensatz zu einem drei-dimensionalen Polyanion in den Verbindungen $CaTIn_2$, $CaTSn_2$ und $SrTIn_2$. Semi-empirische Bandstrukturrechnungen sind im Einklang mit einem zweidimensionalen Polyanion, in dem die stärksten Wechselwirkungen für die T-In Kontakte gefunden wurden.*

Electronic structure calculations: Three-dimensional semiempirical band structure calculations for $BaRhIn_2$ and $BaPtIn_2$ were based on an extended Hückel Hamiltonian.[19, 20] All exchange integrals, orbital exponents and weighting coefficients are listed in Table 2. Charge iterations have been carried out. The eigenvalue problem was solved in reciprocal space at 144 k points within the irreducible wedge of the Brillouin zone by using the YAeHMOP code.[21]

Results and Discussion

Lattice parameters: Already the trend in volume of the unit cells (Figure 1) reveals a discontinuity when the metallic single bond radii are compared.[22] One would expect that the

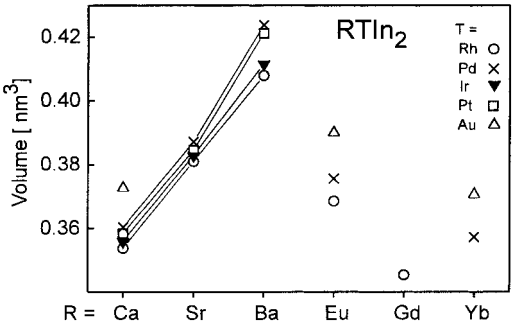

Figure 1. Volumes of the unit cells of some $RTIn_2$ compounds (R = Ca, Sr, Ba, Eu, Gd, Yb) which are isopointal with the $MgCuAl_2$-type structure. Note, that only half the volume is plotted for $CaRhIn_2$ and $CaIrIn_2$.

Rh(Ir) compound should have a larger volume than the Pd(Pt) compound, but only the b lattice parameter follows the course of the radii (Table 1). For the lattice parameter a and the volume one finds that $BaPtIn_2$ has smaller values than the $BaPdIn_2$ compound. A complete reversal of this behavior is observed when the c lattice parameter is considered. The order is Pt-Pd-Ir-Rh which is in contrast to the order of the metallic single bond radii[22] and the radii for coordination number 12[23] for Rh, Pd, Ir, and Pt of 125.2, 128.3, 126.5, and 129.5 pm and of 134.5, 137.6, 135.7, and 138.7 pm, respectively. Thus, the lattice parameters show a remarkable anisotropic behavior. This is associated with the fact that the indium substructure is modified quite significantly depending on the electron count of the transition metal. At the same time the polyanion formed by the transition metal and indium atoms contracts in the a and c direction, while it stretches in the b direction. This is different in gold-containing compounds such as $CaAuIn_2$,[3] $EuAuIn_2$,[24] and $YbAuIn_2$.[25]

The size restrictions implied by the alkaline earth elements calcium, strontium, and barium lead to interesting features. $MgCuAl_2$-type compounds are formed with strontium for Rh, Pd, Ir, and Pt, but the smaller calcium atoms cause the formation of a different structure type for Rh and Ir; that is the $CaRhIn_2$-type.[4] Half the volume of $CaRhIn_2$ and $CaIrIn_2$

Table 2. Crystal data and structure refinements for $BaRhIn_2$ and $BaPtIn_2$.

empirical formula	$BaRhIn_2$	$BaPtIn_2$
molar mass [g mol^{-1}]	469.89	562.07
crystal system	orthorhombic	orthorhombic
space group	*Cmcm* (no. 63)	*Cmcm* (no. 63)
Pearson symbol	oC16	oC16
Z	4	4
unit cell dimensions	Table 1	Table 1
calculated density [g cm^{-3}]	7.65	8.86
crystal size [μm^3]	$15 \times 25 \times 40$	$10 \times 25 \times 35$
transmission ratio [max/min]	1.56	2.35
absorption coefficient [mm^{-1}]	24.4	52.9
$F(000)$	796	928
θ range for data collection	2° to 30°	2° to 30°
range in hkl	$-6 \le k \le 0, \pm 15, \pm 11$	$-2 \le k \le 6, \pm 16, -11 \le l \le 1$
total no. reflections	1168	730
independent reflections	354 ($R_{int} = 0.0461$)	362 ($R_{int} = 0.0295$)
reflections with $I > 2\sigma(I)$	308 ($R_{sigma} = 0.0305$)	312 ($R_{sigma} = 0.0307$)
data/restraints/parameters	354/0/16	362/0/16
goodness-of-fit on F^2	1.134	1.120
final R indices [$I > 2\sigma(I)$]		
$R1$	0.0209	0.0522
$wR2$	0.0527	0.1292
R indices (all data)		
$R1$	0.0288	0.0610
$wR2$	0.0561	0.1427
extinction coefficient	0.0007(2)	0.0012(5)
largest diff. peak and hole [e Å^{-3}]	1.84 and −1.88	6.74 and −9.71

fits very well into the trend observed with respect to the volume of the $MgCuAl_2$-type compounds (Figure 1). Yet the large barium atoms force the structure to expand which is not done in an isotropic way (see above).

Structure refinements: Platelet-like single crystals of $BaRhIn_2$ and $BaPtIn_2$ were isolated from the annealed samples by mechanical fragmentation and were examined by Buerger precession photographs in order to establish both symmetry and suitability for intensity data collection. The photographs showed *C*-centered orthorhombic cells with Laue symmetry *mmm*. The extinction conditions were compatible with space group *Cmcm* in agreement with all previous investigations.[3, 4] All relevant crystallographic data and experimental details for the data collections are listed in Table 3.

The atomic parameters of $SrRhIn_2$[6] were taken as starting values, and the structures were successfully refined using SHELXL-97 (full-matrix least-squares on F^2)[26] with anisotropic atomic displacement parameters for all atoms. Final difference Fourier syntheses revealed no significant residual peaks (see Table 1). The highest residual density of 6.74 e Å^{-3} in $BaPtIn_2$ was too close to the platinum position (70 pm) and most likely resulted from an incomplete absorption correction. The elevated $wR2$ value for $BaPtIn_2$ may be attributed to some deterioration during the data collection and the lesser quality of the single crystal used for the structure refinement. The positional parameters and interatomic distances of the two refinements are listed in Tables 4 and 5, respectively. Listings of the observed and calculated structure factors are available; further details on the crystal structure investigations may be obtained from the Fachinformationszentrum Karlsruhe, 76344 Eggenstein-Leopoldshafen, Germany (fax:

Table 3. Extended Hückel parameters.

Atom	Orbital	H_{ii} (eV)	ξ_1	c_1	ξ_2	c_2
Ba	6s	−4.760	1.263			
	6p	−2.640	1.263			
Rh	5s	−8.090	2.135			
	5p	−4.570	2.100			
	4d	−12.500	4.290	0.581	1.970	0.569
Pt	6s	−9.077	2.554			
	6p	−5.475	2.554			
	5d	−12.590	6.013	0.633	2.696	0.551
In	5s	−12.600	1.903			
	5p	−6.190	1.677			

Table 4. Atomic coordinates and isotropic displacement parameters [pm^2] for $BaRhIn_2$ and $BaPtIn_2$.

Atom	Wyckoff position	x	y	z	U_{eq}[a]
$BaRhIn_2$					
Ba	4*c*	0	0.05236(5)	1/4	104(2)
Rh	4*c*	0	0.78407(7)	1/4	96(2)
In	8*f*	0	0.33582(4)	0.05514(5)	97(2)
$BaPtIn_2$					
Ba	4*c*	0	0.0526(1)	1/4	117(5)
Pt	4*c*	0	0.77635(8)	1/4	95(4)
In	8*f*	0	0.3366(1)	0.0565(2)	104(5)

[a] U_{eq} is defined as one third of the trace of the orthogonalized U_{ij} tensor.

Table 5. Interatomic distances [pm], calculated with the lattice parameters taken from X-ray powder data of $BaRhIn_2$ and $BaPtIn_2$. All distances within the first coordination sphere are listed. Standard deviations are all equal or less than 0.2 pm.

$BaRhIn_2$				$BaPtIn_2$			
Ba:	1	Rh	303.5	Ba:	1	Pt	321.1
	2	Rh	344.7		2	Pt	344.6
	4	In	355.7		4	In	357.9
	2	In	357.0		2	In	364.7
	4	In	367.1		4	In	371.7
	2	Ba	419.9		2	Ba	419.0
Rh:	4	In	279.6	Pt:	2	In	278.6
	2	In	280.7		4	In	282.9
	1	Ba	303.5		1	Ba	321.1
	2	Ba	344.7		2	Ba	344.6
In:	2	Rh	279.6	In:	1	Pt	278.6
	1	Rh	280.7		2	Pt	282.9
	2	In	309.3		1	In	310.1
	1	In	314.0		2	In	315.9
	2	Ba	355.7		2	Ba	357.9
	1	Ba	357.0		1	Ba	364.7
	2	Ba	367.1		2	Ba	371.7
	1	In	381.9		1	In	390.6

0947-6539/01/0702-0384 $ 17.50+.50/0 *Chem. Eur. J.* **2001**, *7*, No. 2

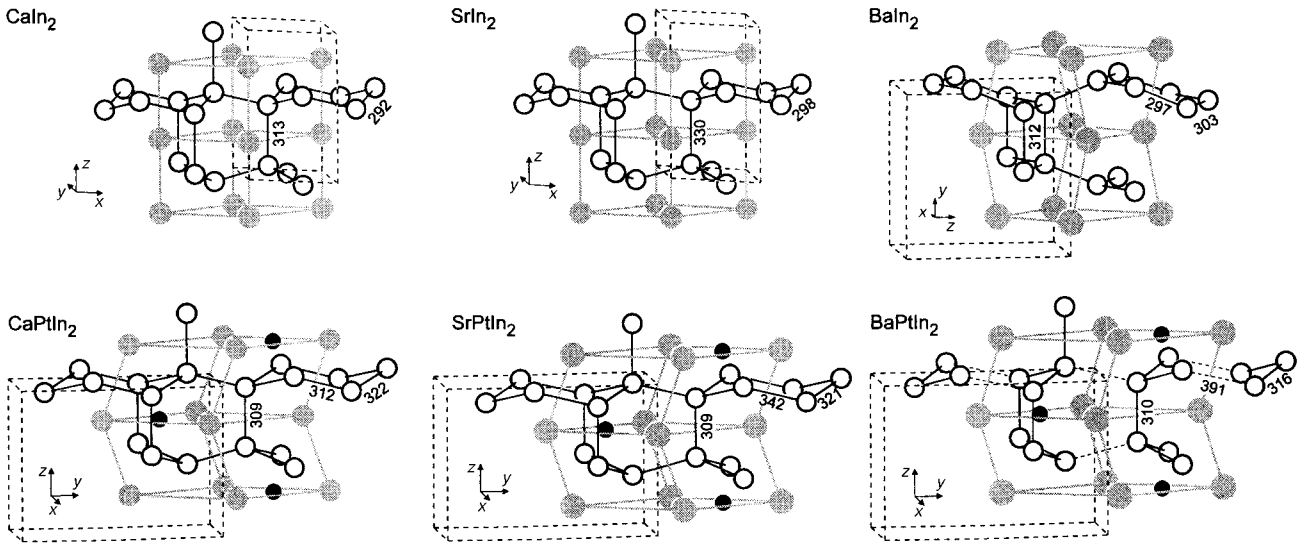

Figure 2. Cutouts of $AEIn_2$ (AE = Ca, Sr, Ba) and $AEPtIn_2$ structures. Large grey, medium open, and black filled circles represent AE, platinum and indium, respectively. Selected bond lengths within the indium networks are given in pm.

(+49) 7247-808-666; e-mail: crysdata@fiz-karlsruhe.de), on quoting the depository numbers CSD-411229 ($BaRhIn_2$) and CSD-411228 ($BaPtIn_2$).

Crystal chemistry and chemical bonding: The new ternary compounds $BaTIn_2$ (T = Rh, Pd, Ir, Pt) are isopointal[27, 28] to the $MgCuAl_2$ structure. $CaTIn_2$ (T = Pd, Pt, Au) and $SrTIn_2$ (T = Rh, Pd, Ir, Pt) crystallize also with the $MgCuAl_2$-type structure and can be described as transition metal filled variants of the Zintl phases $CaIn_2$ or $SrIn_2$. Thus a one-step symmetry reduction from the hexagonal space group $P6_3/mmc$ of $CaIn_2$ to $Cmcm$ of orthorhombic $AETIn_2$ (AE = Ca, Sr, Ba) can be applied. Cutouts of these structures are shown in Figure 2. The indium substructures have the same topology as hexagonal diamond[27] (lonsdaleite). The four-connected indium network implies an In^- according to the Zintl–Klemm concept. The In–In distances within the indium network strongly depend on the size of the cations and on the electron count of the transition metal.[4–6] With barium as the least electronegative component they also resemble a series with the largest possible cation (except radium) at the magnesium position. The volume of the compounds with the 2+ cations europium and ytterbium is similar to that of the strontium and calcium compounds,[24, 25] respectively (Figure 1).

The near-neighbor environments in the compounds $AETIn_2$ do not change very much within the series AE = Ca, Sr, and Ba despite the increasing atomic size. The lengthening of the *b* lattice parameter, of course, leads to rather strong distortions. The discussion of the coordination spheres is exemplified by using $BaPtIn_2$. The barium atoms have the coordination number 13 (10 In+3 Pt). The average Ba–Pt distance of 337 pm is longer than the sum of Pauling's single bond radii of 328 pm, but is still shorter than the sum of the radii for coordination number 12 (363 pm). The Ba–In distances show the same tendencies. Even though the Ba–Pt and Ba–In distances are quite long, one still has to assume that bonding Ba–Pt and Ba–In interactions exist. Both contacts are weak, but they are essential for the linkage of the polyanion in the *b* direction.

The transition metals have coordination number 9 (6 In+3 Ba). Four indium and two barium atoms form a trigonal prism which is augmented by two indium and one barium atom on the rectangular faces. The indium atoms have coordination number 11 (5 Ba, 3 Pt, 3 In).

The shortest distances occur for the Pt–In contacts (av 281 pm) and these agree well with the sum of Pauling's single bond radii of 279 pm. This is an overall trend for the series $AETIn_2$ (A = Ca, Sr, Ba; T = Rh, Pd, Ir, Pt) and supports the assumption of rather rigid transition metal indium contacts. The size of the barium atoms puts a large tension on the polyanion as is expressed by the interatomic distances (Table 5). This has significant consequences for the polyanions formed by the transition metal and indium atoms, but has an even greater influence on the pseudohexagonal indium network. The structure does not simply expand isotropically in going from calcium and strontium to barium: In order to maintain an optimized $[TIn_2]$ polyanion, the increasing space requirement of calcium, strontium, and barium is counteracted by gradually breaking apart the indium network by the lengthening of the In–In distance which is approximately parallel to the *b* axis. Thus, the three-dimensional polyanion is transformed to a mere two-dimensional polyanion (Figure 3).

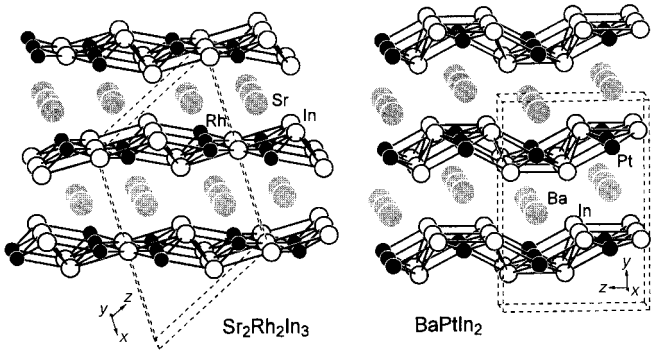

Figure 3. The two-dimensional polyanions $[Rh_2In_3]$ and $[PtIn_2]$ in the structures of $Sr_2Rh_2In_3$ (left) and $BaPtIn_2$ (right). Large gray, medium open, and black filled circles represent Sr(Ba), Rh(Pt), and In, respectively.

Simultaneously, the T–In contacts remain close to the respective sum of Pauling's single bond radii. Thus, the contacts between the transition metal and indium are predominant in the structure. A similar two-dimensional polyanion was recently observed in the compound $Sr_2Rh_2In_3$.[16] The volume change (Figure 1) reflects this anisotropic indium–indium distance modulation. Owing to the anisotropic behavior the ratios of the axes are quite different from those of the $MgCuAl_2$-type structure, and the structure of $BaTIn_2$ is better referred to as being isopointal to $MgCuAl_2$ rather than isotypic.[27, 28]

Semiempirical band structure calculations were carried out to investigate the $[TIn_2]$ polyanions and the indium substructures in greater detail. The DOS (density of states) curves of $BaRhIn_2$ and $BaPtIn_2$ are very similar to those obtained for the other $MgCuAl_2$-type indides and stannides ($CaTIn_2$, $CaTSn_2$, $SrTIn_2$). Narrow low-lying transition metal *d* bands which are localized around -10 to -13 eV (Figure 4) are characteristic of these structures. The indium states spread out over the whole energy range. The contributions of the cations (calcium, strontium, barium) are negligible below the Fermi level leading to the formulation $Ba^{2+}[TIn_2]^{2-}$. This is also supported by the gross Mulliken charges (Table 6). By comparing the DOS of the binary $BaIn_2$[11] with that of $BaRhIn_2$ and $BaPtIn_2$, one finds the gap closed and the Fermi level decreased as can be expected considering the insertion of transition metal atoms.

Some words of caution seem to be appropriate at this point. The electronic structures of these barium compounds, especially those with platinum and iridium as the transition metal component are certainly influenced by relativistic effects which might affect the overlap populations and the Mulliken charges. Nevertheless, in a recent paper[3] we investigated the $CaTIn_2$ (T = Pd, Pt, Au) structures both by extended Hückel and ab initio TB-LMTO-ASA band structure calculations. It turned out that the electronic structure is qualitatively the same considering the tendencies in chemical bonding. We can thus discuss a qualitative bonding scheme for the series of isotypic $BaTIn_2$ compounds on the basis of the extended Hückel results.

The insertion of transition metals corresponds to an at least partial oxidation of the indium substructure. This is also suggested by the course of the absolute electronegativities according to Pearson[30] (barium 2.4 eV, platinum 5.6 eV, and indium 3.1 eV). Thus, the *d* orbitals of the transition metals are filled. By analyzing the semiempirical crystal orbital overlap populations (COOP, Figure 4 and Table 6) it is revealed that electron density is transferred from the implied In^- to the transition metal atoms, as is apparent from the large positive overlap population for the platinum–indium and indium–indium contacts (upper right hand corner of Figure 4.) It is notable that these COOP curves still show bonding contributions above the Fermi level. However, it seems unlikely that these states might be filled, because at the same time antibonding In–In states will be filled (middle part of Figure 4) which belong to the In–In bonds within the puckered indium hexagons (Figure 2).

The difference in bond strength of the four In–In contacts in $BaPtIn_2$ is seen by analyzing the COOP curves for the long

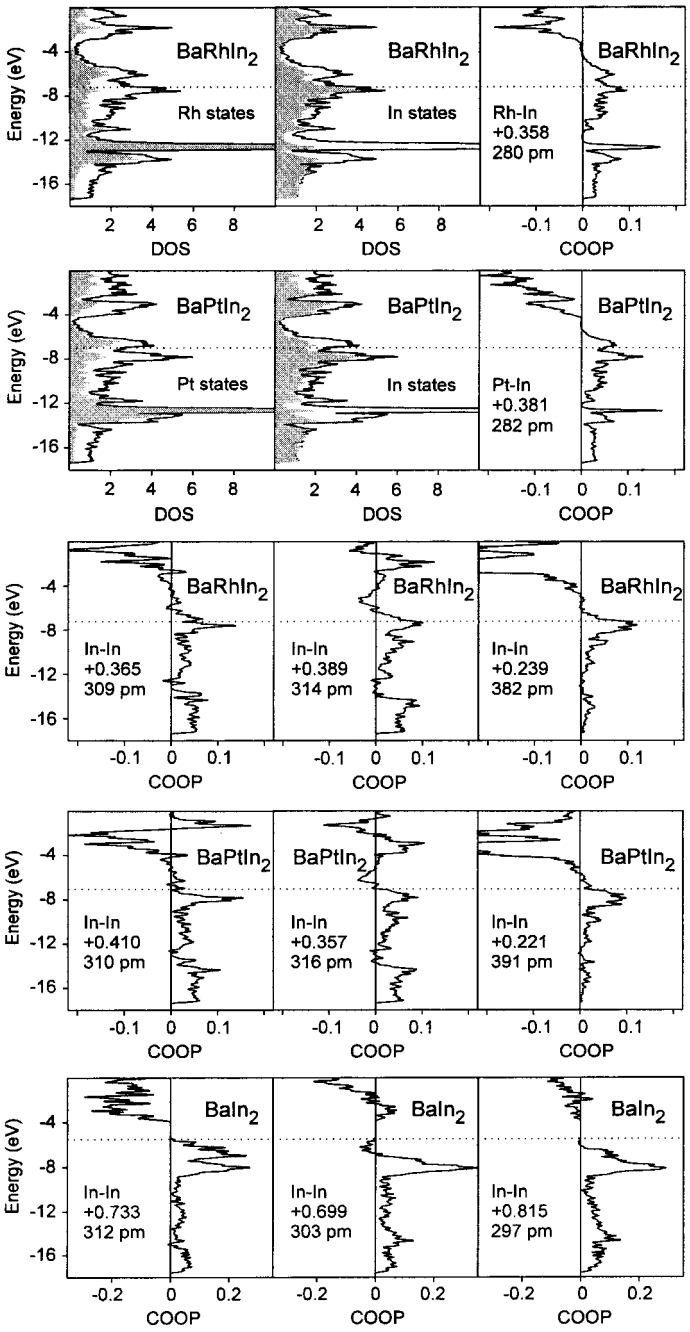

Figure 4. Total and projected density-of-states (DOS) curves for $BaRhIn_2$ and $BaPtIn_2$ and selected crystal orbital overlap population (COOP) curves for $BaRhIn_2$, $BaPtIn_2$, and $BaIn_2$. The rhodium and platinum contributions are shaded. The integrated values for the overlap population per bond up to the Fermi level (dotted line) and the corresponding distances are given.

In–In distance of 391 pm in comparison to the shorter In–In interactions within the two-dimensional $[TIn_2]$ polyanion. The integrated overlap population is significantly smaller (Table 6). Even though the indium substructure is stretched along the *b* direction, the COOP curves of the three different In–In contacts still look very much like those of binary $BaIn_2$[11] (lower part of Figure 4). One difference, however, is the lower Fermi level in the ternary compounds which lets these antibonding states lie above the Fermi level. One might think of the $BaIn_2$ structure as a compromise between an environ-

0947-6539/01/0702-0386 $ 17.50+.50/0 *Chem. Eur. J.* **2001**, *7*, No. 2

Table 6. Net charges (q) and crystal orbital overlap (OP) populations for $BaRhIn_2$ and $BaPtIn_2$ as obtained from the extended Hückel calculations. T denotes the respective transition metal. The In–In bond lengths are given in parentheses for each overlap population.

Parameter	$BaRhIn_2$	$BaPtIn_2$
q (Ba)	+2.04	+1.98
q (T)	−2.06	−1.82
q (In)	+0.01	−0.08
OP (Ba–T)	−0.039	−0.034
OP (Ba–In)	−0.023	−0.017
OP (T–In)	+0.358	+0.381
OP (In–In)	+0.365	+0.410
	(309 pm)	(310 pm)
OP (In–In)	+0.389	+0.357
	(314 pm)	(316 pm)
OP (In–In)	+0.239	+0.221
	(382 pm)	(391 pm)

ment large enough for the barium atoms and the formation of a pseudo-hexagonal indium sublattice at the cost of the occupancy of antibonding states.

One draw back of the extended Hückel calculation might be the fact that the structures of the series $CaTIn_2$, $SrTIn_2$, and $BaTIn_2$ become more ionic. This makes the value of the overlap populations for the In–In contacts in $BaIn_2$ very large.[11] In the ternary compounds, however, this effect is not observed, but still one can assume that the large polarizability of barium in comparison to calcium and strontium may be held responsible for the formation of a two-dimensional polyanion. The relatively low polarizability of calcium in $CaRhIn_2$ and $CaIrIn_2$,[4] however, leads to a complex three-dimensional polyanionic network. The strontium compounds of the $MgCuAl_2$-type structure, on the other hand, resemble the best compromise for an optimized polyanion and a diamond-like indium substructure. The tendency toward a two-dimensional polyanion, however, is already present if one compares the increase of the "interlayer" In–In distance of 312 pm for $CaPtIn_2$, 342 pm for $SrPtIn_2$, and 391 pm for $BaPtIn_2$ (Figure 2).

One may speculate about the existence of a low-temperature form of $BaTIn_2$ which should be derived from the orthorhombic KHg_2-type $BaIn_2$ rather than from the hexagonal $CaIn_2$ type. But it is more probable that a high-pressure form of $BaIn_2$ with the hexagonal $CaIn_2$ type might exist with a more isotropic structure and a compressed diamond-like indium network with more regular tetrahedra.

Acknowledgement

We are indebted to Dipl.-Ing. U. C. Rodewald for the intensity data collections, to H.-J. Göcke for the EDX analyses and to the Degussa-Hüls AG for a generous gift of noble metals. This work was financially supported by the Fonds der Chemischen Industrie and the Deutsche Forschungsgemeinschaft.

[1] V. I. Zaremba, O. Ya. Zakharko, Ya. M. Kalychak, O. I. Bodak, *Dopov. Akad. Nauk. Ukr. RSR, Ser. B* **1987**, 44.
[2] L. V. Sysa, Ya. M. Kalychak, *Crystallogr. Rep*. **1993**, *38*, 278.
[3] R.-D. Hoffmann, R. Pöttgen, G. A. Landrum, R. Dronskowski, B. Künnen, G. Kotzyba, *Z. Anorg. Allg. Chem*. **1999**, *625*, 789.
[4] R.-D. Hoffmann, R. Pöttgen, *Z. Anorg. Allg. Chem*. **2000**, *626*, 28.
[5] R.-D. Hoffmann, D. Kußmann, U. C. Rodewald, R. Pöttgen, C. Rosenhahn, D. Mosel, *Z. Naturforsch. Teil B* **1999**, *54*, 709.
[6] R.-D. Hoffmann, U. C. Rodewald, R. Pöttgen, *Z. Naturforsch. B* **1999**, *54*, 38.
[7] B. Aronsson, M. Bäckman, S. Rundqvist, *Acta Chem. Scand*. **1960**, *14*, 1001.
[8] H. Perlitz, A. Westgren, *Ark. Kemi*, *Mineral. Geol*. **1943**, *16*, 1.
[9] A. Iandelli, *Z. Anorg. Allg. Chem*. **1964**, *330*, 221.
[10] G. Bruzzone, G. B. Bonino, *Atti Accad. Nat. Lincei* **1970**, *48*, 235.
[11] G. Nuspl, K. Polborn, J. Evers, G. A. Landrum, R. Hoffmann, *Inorg. Chem*. **1996**, *35*, 6922.
[12] E. J. Duwell, N. C. Baenziger, *Acta Crystallogr*. **1955**, *8,* 705.
[13] A. C. Larson, D. T. Cromer, *Acta Crystallogr*. **1961**, *14,* 73.
[14] R. Pöttgen, T. Gulden, A. Simon, *GIT Labor-Fachzeitschrift* **1999**, *33*, 143.
[15] R. Pöttgen, A. Lang, R.-D. Hoffmann, B. Künnen, G. Kotzyba, R. Müllmann, B. D. Mosel, C. Rosenhahn, *Z. Kristallogr*. **1999**, *214*, 143.
[16] R.-D. Hoffmann, D. Kußmann, R. Pöttgen, *J. Inorg. Mater*. **2000**, *2*, 135.
[17] R.-D. Hoffmann, R. Pöttgen, unpublished results.
[18] K. Yvon, W. Jeitschko, E. Parthé, *J. Appl. Crystallogr*. **1977**, *10*, 73.
[19] R. Hoffmann, *J. Chem. Phys.* **1963**, *39*, 1397.
[20] R. Hoffmann, *Solids and Surfaces: A Chemist's View of Bonding in Extended Structures*, VCH, New York, **1988**.
[21] G. A. Landrum, YAeHMOP - Yet Another extended Hückel Molecular Orbital Package, Version 2.0, **1997**; available on: http://overlap.chem.cornell.edu:8080/yaehmop.html.
[22] L. Pauling, *The Nature of the Chemical Bond and the Structure of Molecules and Crystals,* Cornell University Press, Ithaca, NY, **1960**.
[23] E. Teatum, K. Gschneidner, Jr., J. Waber, Rep. LA-2345, US Department of Commerce, Washington, DC, **1960**.
[24] R.-D. Hoffmann, R. Pöttgen, *Z. Kristallogr.*, **2000**, *Suppl. 17*, 121.
[25] Ya. V. Galadzhun, R.-D. Hoffmann, G. Kotzyba, B. Künnen, R. Pöttgen, *Eur. J. Inorg. Chem.* **1999**, 975.
[26] G. M. Sheldrick, SHELXL-97, Program for Crystal Structure Refinement, University of Göttingen, Germany, **1997**.
[27] L. M. Gelato, E. Parthé, *J. Appl. Crystallogr*. **1987**, *20*, 139.
[28] E. Parthé, L. M. Gelato, *Acta Crystallogr. Sect. A*. **1984**, *40*, 169.
[29] J. Donohue, *The Structures of the Elements*, Wiley, New York, **1974**.
[30] R. G. Pearson, Inorg. Chem. **1988**, *27*, 734.

Received: April 11, 2000 [F2415]